

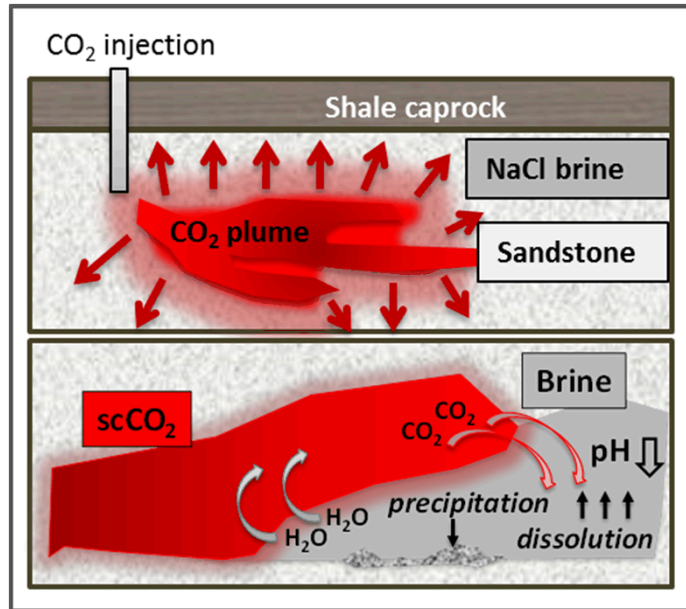
Geologic sequestration of CO₂: mineral dissolution and precipitation during CO₂ injection at the Frio-I brine pilot

Anastasia G. Ilgen

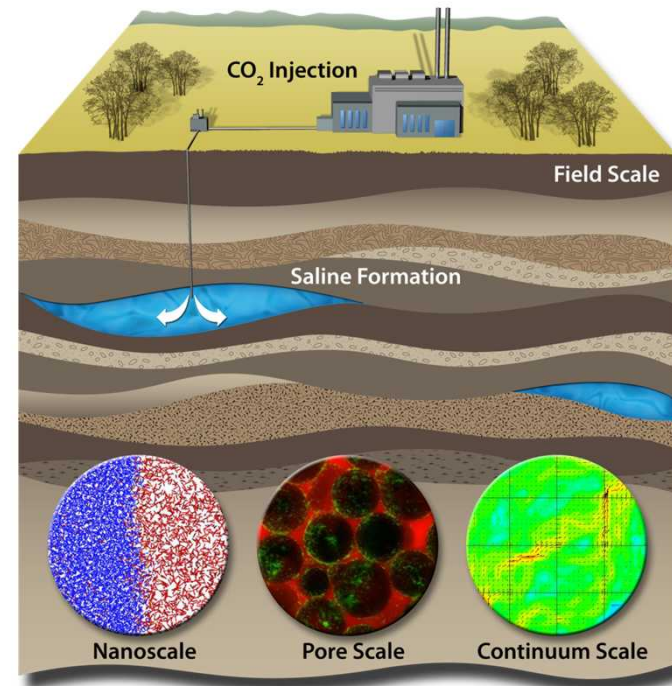
November 12, 2014

Outline

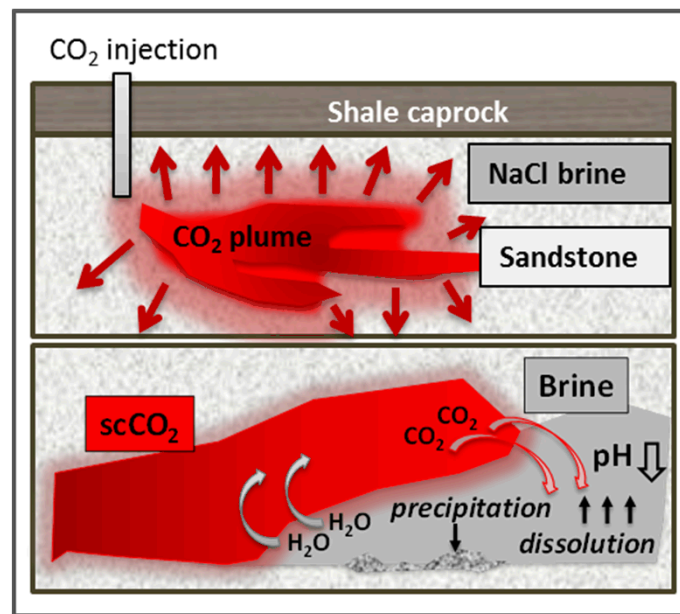
Mineral Dissolution and Precipitation during CO₂ Injection at the Frio-I Brine Pilot



Overview Center for Frontiers of Subsurface Energy Security (CFSES)

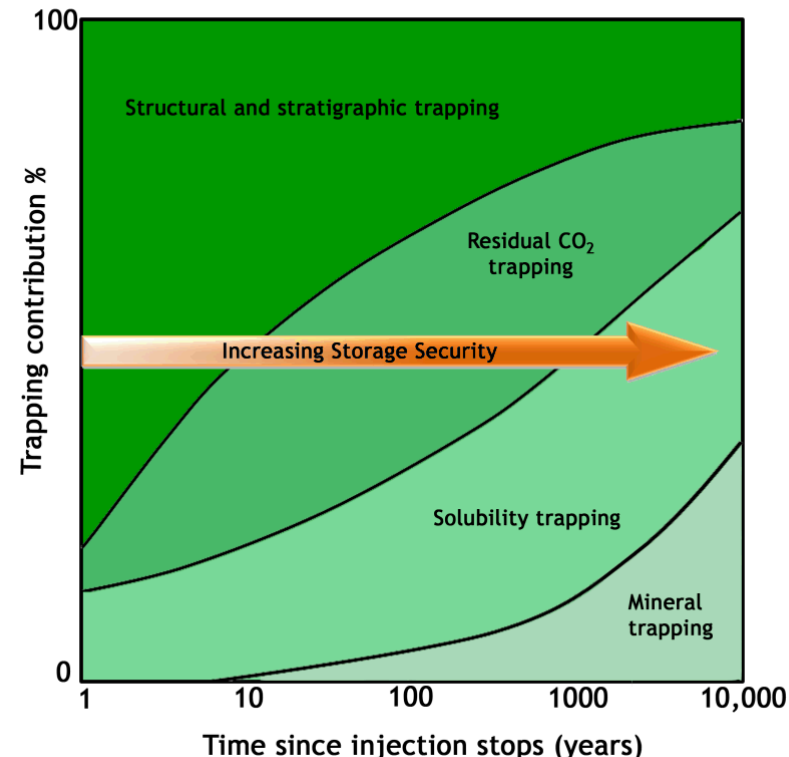


Mineral Dissolution and Precipitation during CO₂ Injection at the Frio-I Brine Pilot: Geochemical Modeling and Uncertainty Analysis



Geologic sequestration of CO₂

- Feasible methods for decreasing atmospheric carbon dioxide (CO₂). ¹⁻⁵
- Natural analogs for CO₂ storage are stable and retain CO₂ on geologic time scales. ²
- Solubility trapping is the predominant CO₂ sink. ⁶
- Crucial features: sufficient porosity, and continuous and fracture-free cap rock.
- Deep saline reservoirs - one of the top candidate formations for geologic storage of CO₂. ^{1, 2}



[1] DePaolo et al., 2013

[2] Marini, 2006

[3] Kharaka and Cole, 2011

[4] Kobos et al., 2011

[5] Steele-MacInnis et al., 2012

[6] Gilfillan et al., 2009

Geochemical response triggered by the injection of CO₂

- At the deep geologic storage PT: CO₂ is stable in its supercritical (sc) state.
- scCO₂ stimulates **geochemical responses**: acidification of parent brine, and dehydration of mineral surfaces by the dispersing scCO₂ phase.^{1-3, 8}
- Experimental and field studies: geochemical reactions differ significantly for different rock assemblages and brine compositions.⁷⁻⁹
- Typical low-permeability cap rocks (e.g. shale) are reactive at the higher end of the geologic carbon storage temperature range.^{10, 11}
 - Dissolution and re-precipitation of **carbonate minerals**, dissolution of **feldspars**, and precipitation of **clay minerals**.¹⁰
- Dissolution and secondary mineral precipitation control the evolution of **porosity** and **permeability**⁸, with potential impact on the cap rock integrity, and CO₂ leakage.^{10, 12}

[1] DePaolo et al., 2013

[2] Marini, 2006

[3] Kharaka and Cole, 2011

[4] Kobos et al., 2011

[5] Steele-MacInnis et al., 2012

[6] Gilfillan et al., 2009

[7] Bickle et al., 2013

[8] Jun et al., 2012

[9] Lu et al., 2012

[10] Liu et al., 2012

[11] Kaszuba et al., 2003

[12] Harvey et al., 2012

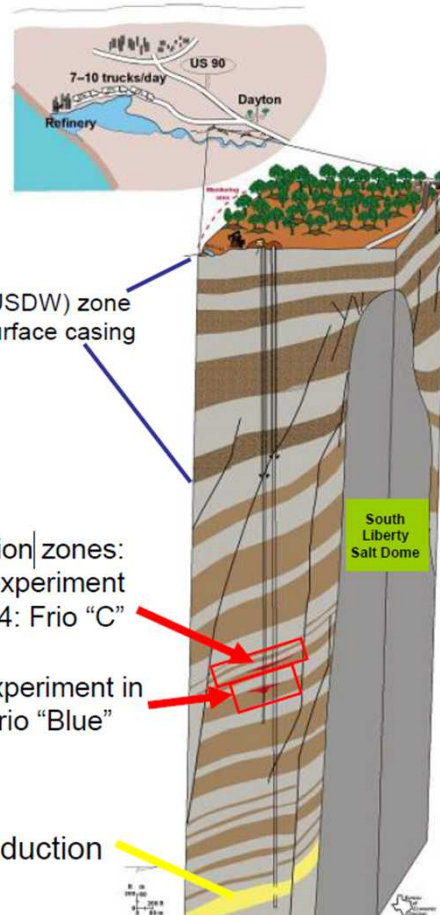


Figure from presentation by T. Meckel (2008)

Frio-I Pilot in 2004

- Setting: salt dome flank, Frio sandstone;
- 1600 tons at 3 kg/s, 10 day injection in 1545 m deep well;
- ~ 40 water samples collected for 4 days using 1530 m deep monitoring well.

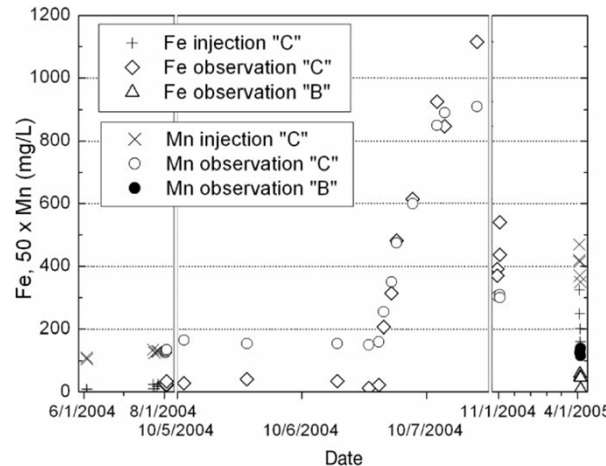
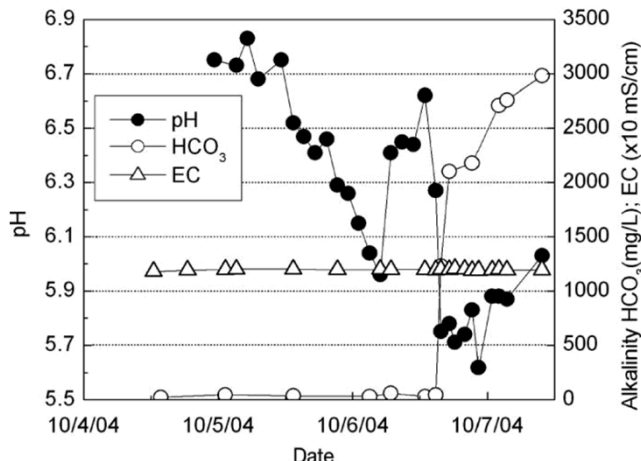
Water chemistry

Component	Concentration (mol/kg H ₂ O)
Ca ²⁺	6.6×10^{-2}
Mg ²⁺	2.2×10^{-2}
Na ⁺	1.35
K ⁺	4.53×10^{-3}
Iron	4.63×10^{-4}
SiO ₂ (aq)	2.50×10^{-4}
Carbon	5.04×10^{-2}
Sulfur	4.20×10^{-5}
Al ³⁺	1.56×10^{-8}
Cl ⁻	1.49
O ₂ (aq)	4.88×10^{-68}
pH	6.7
Temperature	59 °C

Minerals

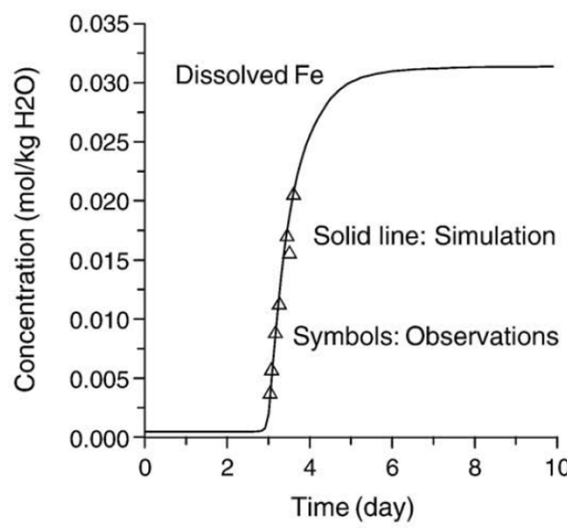
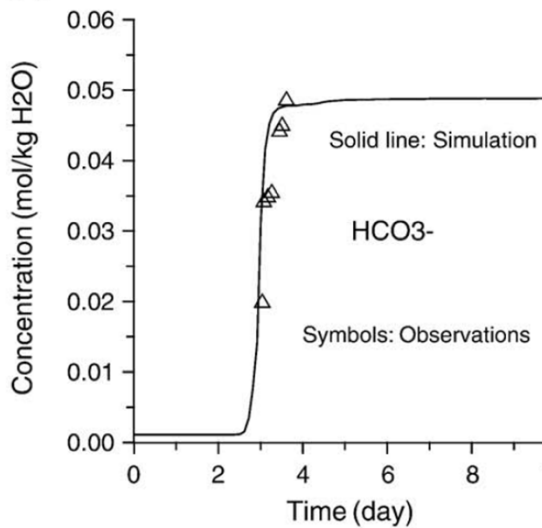
Quartz	Oligoclase	Illite
Kaolinite	K-feldspar	Na-smectite
Calcite	Chlorite	Hematite

Water chemistry observations and modeling



- pH drop \downarrow 6.5 to 5.7;
- Alkalinity \uparrow 100 to 1100 mg/L;
- Fe \uparrow 30 to 1100 mg/L;
- Mn and Ca \uparrow

Figures from Kharaka et al. (2006) *Geology*, 34, 577

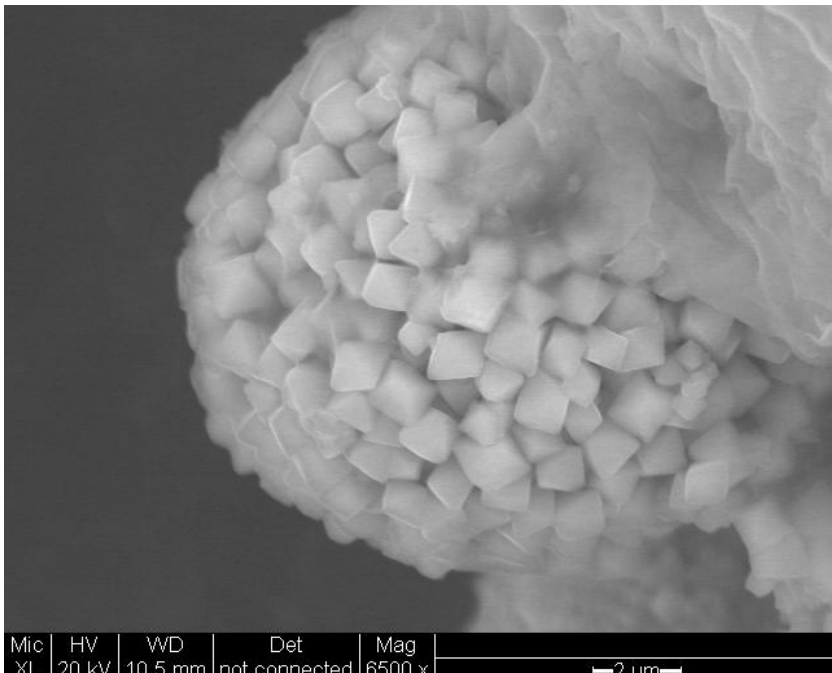


- Existing models capture changes in inorganic chemistry, Fe in particular, in the observation well over time.
- Conclude: fast dissolution of calcite and Fe oxide.

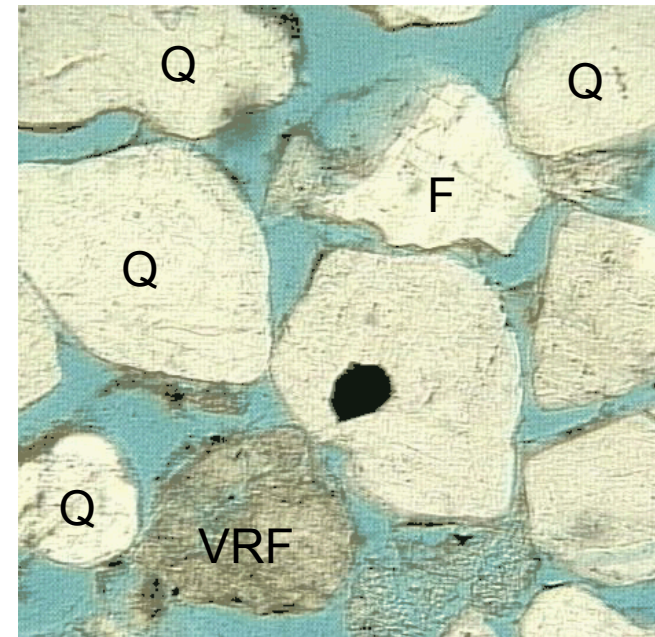
Figures from Xu et al. (2010) *Chem. Geol.*, 271, 153

Petrographic observations

- Calcite cement in Frio Formation varies and can be absent.
- Petrographic study of the Upper Frio Formation “C” found no calcite cement.
- Frio Formation “C” sandstone contains 24 wt. % of feldspar, mostly **anorthite** $\text{CaAl}_2\text{Si}_2\text{O}_8$.



Framboidal pyrite



Quartz (Q), feldspar (F), and volcanic rock fragments (VRF)

- No crystalline iron oxyhydroxides.²³
- Abundant fine-crystalline **pyrite** FeS_2 .²³

Images from McGuire (2009) MS thesis: “CO₂ Injection and Reservoir Characterization: an Integrated Petrographic and Geochemical Study of the Frio Formation, Texas.

Objectives:

- To test the hypothesis that increase in **iron** could be due to the dissolution of pyrite; and increase in **calcium** - to the dissolution of anorthite.
- If dissolution of pyrite and anorthite were likely, incorporate these reactions into the **long-term (1000 years) reactive transport model** to account for precipitation of carbonates (specifically, calcite and siderite).
- Explore the range of **uncertainty** due to indeterminate rate constants for the pyrite, calcite, and anorthite dissolution, and compare the range of predicted values to the actual observations recorded during the Frio-I Brine Pilot.

Method:

- Path of reaction and reactive transport modeling using Geochemists Work Bench (Bethke, 1998).

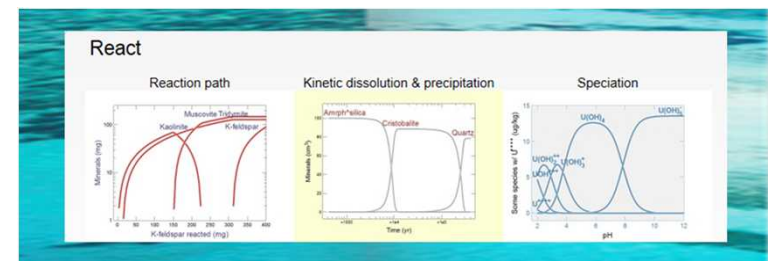


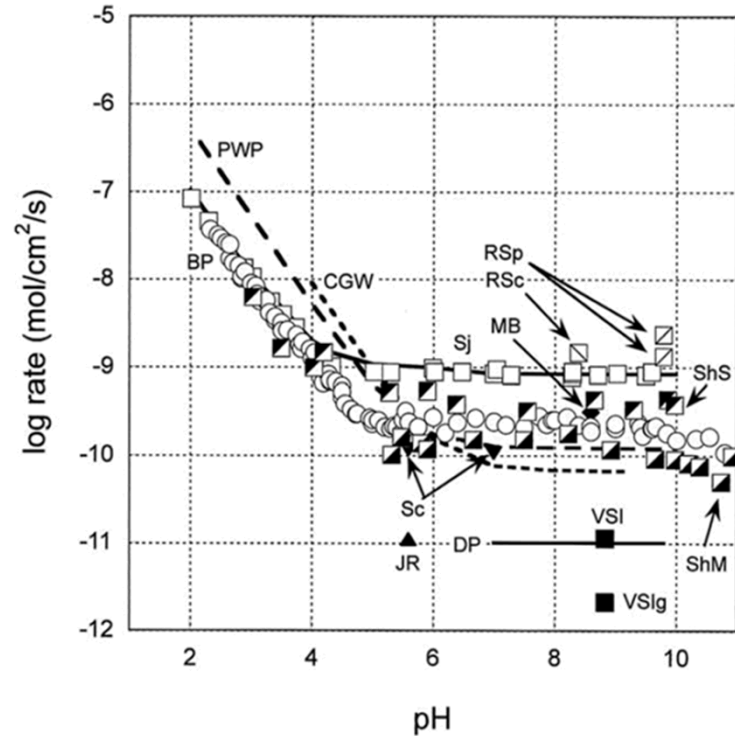
Image source: <http://www.gwb.com/>

Challenges in geochemical modeling of geologic CO₂ sequestration

Marini L. (2007) *Geological Sequestration of Carbon Dioxide: Thermodynamics, Kinetics, and Reaction Path Modeling.*

- Inadequate **activity** correction;
- Unknown **thermodynamic properties** of relevant mineral phases;
- Uncertain reaction **kinetics**;
- Deficiencies in knowledge of **nucleation** and crystal growth;
- Uncertain reactive **surface areas**.

Calcite dissolution rates



Arvidson et al. (2003) *Geochimica et Cosmochimica Acta*, 67, 8, 1623

Activity correction

$$\mu_i \equiv \frac{\partial G_i}{\partial n_i} = \mu_i^{\circ} + RT_K \ln \gamma_i m_i$$

Debye-Hückel methods
Works for $I < 0.1 \text{ m}$

$$\log \gamma_i = -\frac{Az_i^2 \sqrt{I}}{1 + \ddot{a}_i B \sqrt{I}}$$

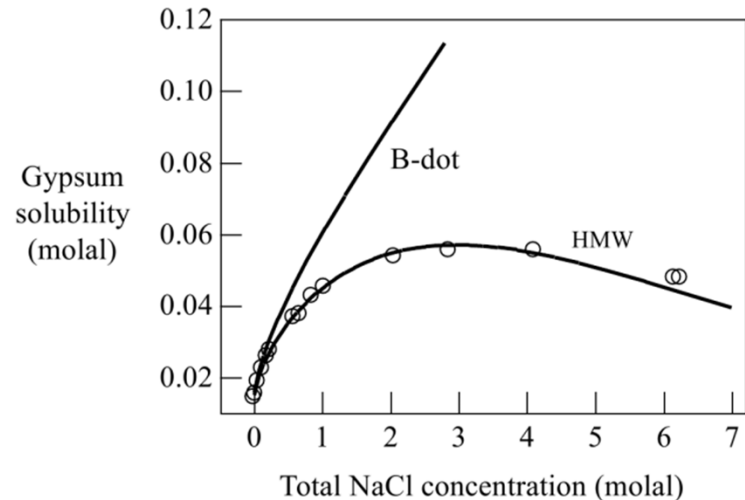
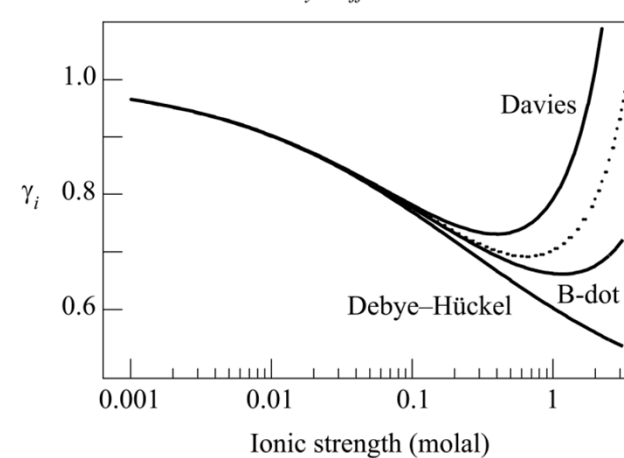
Davies method
Works for $I = 0.3-0.5 \text{ m}$

$$\log \gamma_i = -Az_i^2 \left(\frac{\sqrt{I}}{1 + \sqrt{I}} - 0.3I \right)$$

B-dot method
Works for $I = 0 - 3 \text{ m Na}^+$ and Cl^- ,
 $0.3 - 1 \text{ m other ions}$

$$\log \gamma_i = -\frac{Az_i^2 \sqrt{I}}{1 + a_i B \sqrt{I}} + \dot{B}I$$

Virial methods $\ln \gamma_i = \ln \gamma_i^{\text{dh}} + \sum_j D_{ij}(I)m_j + \sum_j \sum_k E_{ijk}m_j m_k$ \leftarrow e.g. Harvie-Møller-Weare (HMW)



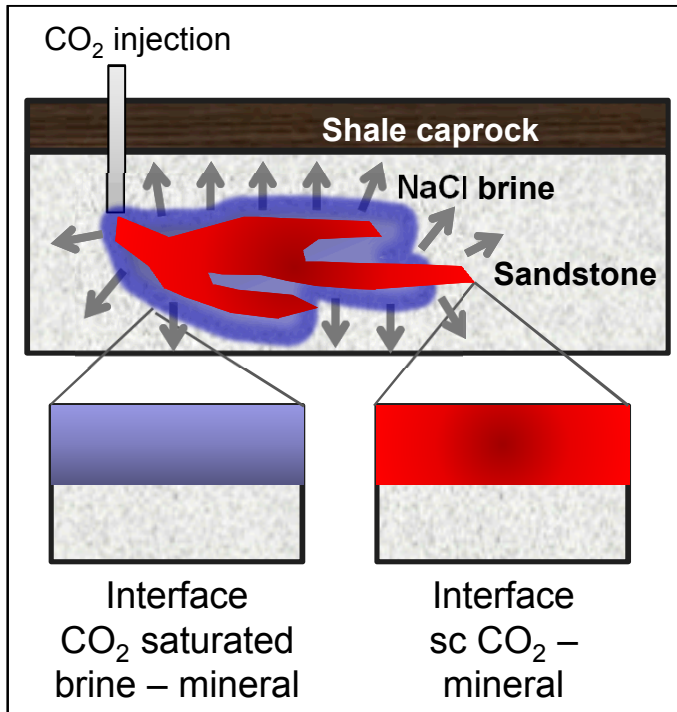
Updated thermodynamic database

- Modified EQ3/6 v. 8.0 (*Wolery, 1992*). Pitzer activity correction method.
- 20 elements: O, Al, B, Br, C, Ca, Cd, Cl, F, Fe, H, K, Li, Mg, Mn, **N**, Na, **P**, S, Si.
- Updated carbonate solubility:
 - ✓ dolomite (Holland and Powell, 1998);
 - ✓ magnesite (Holland and Powell, 1998);
 - ✓ hydromagnesite (Robie and Hemingway, 1995);
 - ✓ dawsonite (Benezeth et al. 2007);
 - ✓ siderite (Benezeth et al. 2009);
 - ✓ added ankerite (Holland and Powell, 1998);
 - ✓ ΔG and ΔH values for HCO_3^- species from (Robie and Hemingway, 1995).

Pitzer parameters are represented by the four term temperature function given by:

$$x(T) = a1 + a2 \times (1/T - 1/298.15) + a3 \times \ln(T/298.15) + a4 \times (T - 298.15) \quad (1)$$

where T is temperature in Kelvin and a1 through a4 denote the temperature function fitting coefficients for the temperature dependent Pitzer parameters.



CO₂ injection creates
two new distinct geochemical interfaces:

1) Supercritical CO₂ – mineral interface:

H₂O activity is decreasing

2) CO₂ saturated brine – mineral:

CO₂(aq) is increasing

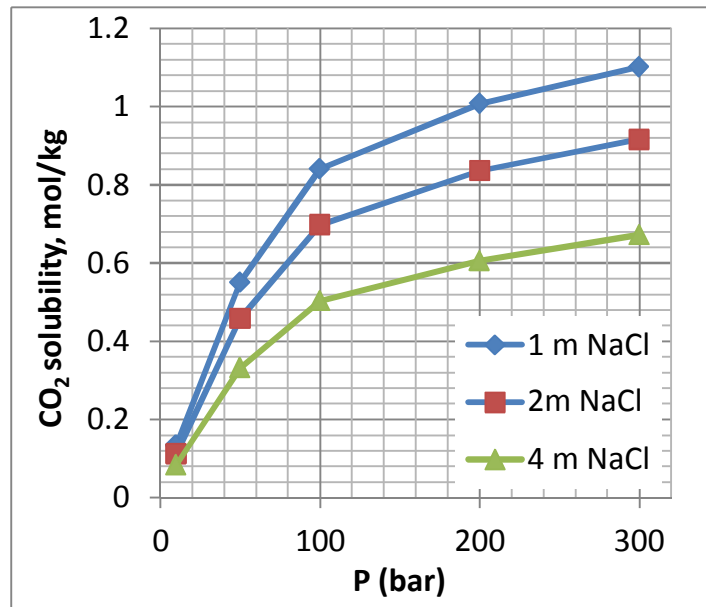
Reaction Path Modeling

Goal: Configure models to predict shifts in pH and mineral saturation

- Aqueous + mineral components, sweep along increasing dissolved CO₂
- Aqueous + mineral components, constant aq. CO₂ and sweep along decreasing H₂O.



Boundary condition 1: Solubility of CO₂ in brine

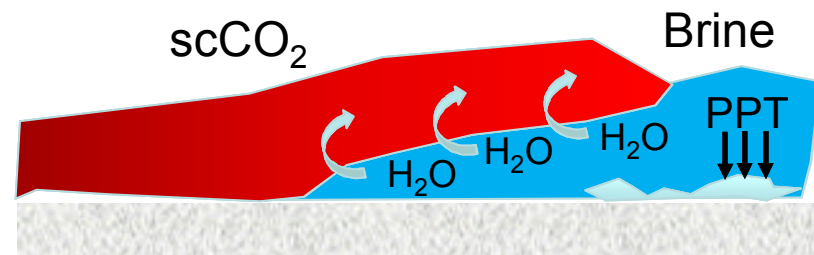


Duan and Sun (2003) *Chem Geo* 193, 257

- Estimated CO₂ solubility at 333.15 K, 150 bar, 1.6 M NaCl
0.82 M



Boundary condition 2: amount of H₂O available after the system is dehydrated due to CO₂ injection



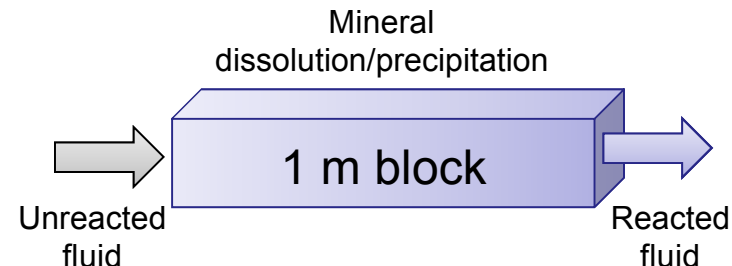
- Assumed maximum 90 wt. % of H₂O is removed due to “drying” by CO₂



Reactive Flow Model

Goal:

To predict long-term mineral dissolution and precipitation after the emplacement of CO₂ in the geochemical conditions representative of the Frio Formation “C” reservoir.



Typical solids and parameters

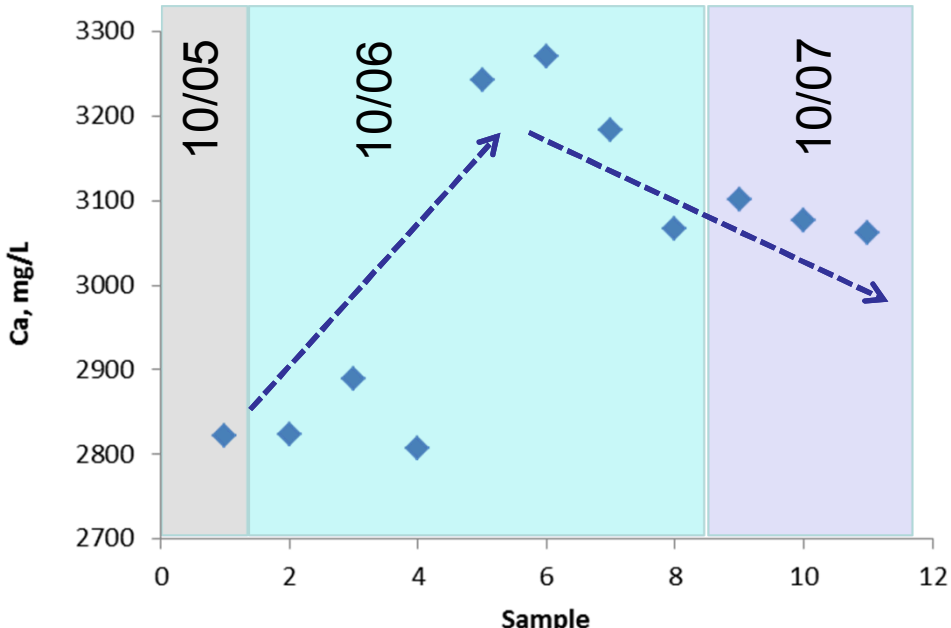
Mineral	Specific surface area cm ² /g	Kinetic rate constant mol/cm ² sec
Calcite	9.8	$5.012 \cdot 10^{-10}$
Quartz	9.8	$1.023 \cdot 10^{-18}$
Kaolinite	151.6	$6.918 \cdot 10^{-18}$
K-feldspar	9.8	$3.89 \cdot 10^{-17}$
Albite	9.8	$1.445 \cdot 10^{-16}$

Values adapted from Xu et al., 2010, values for albite are assumed equal to oligoclase.

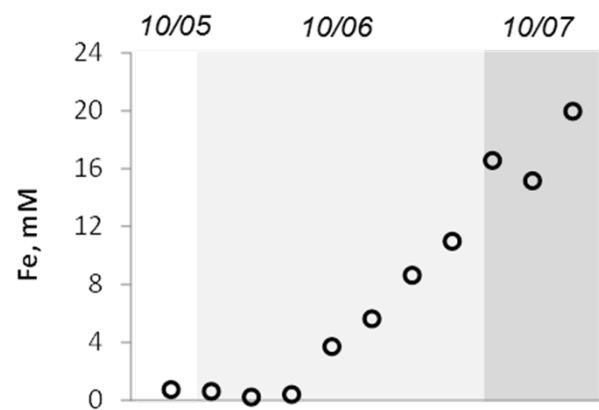
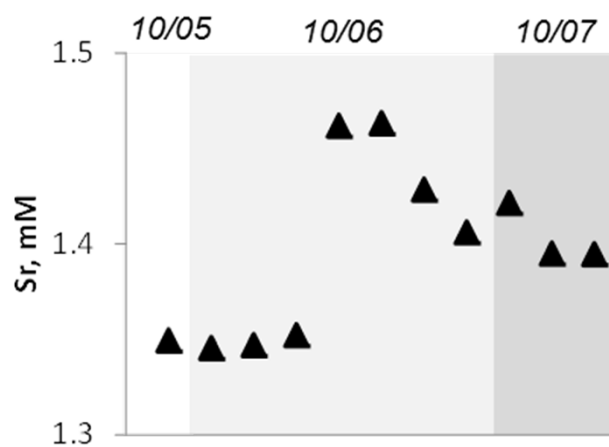
- 1-D Reactive Flow Model
- 1 m block, 23 % porosity
- Initial brine composition of Frio reservoir
- Temperature 25 °C
- Time 1000 years
- Reacting fluid – Frio brine saturated with CO₂(g): 0.82 M HCO₃⁻, pH = 3.3
- Over the course of the simulation pH is allowed to rise back to 7.

Results: Calcium and iron in brine samples

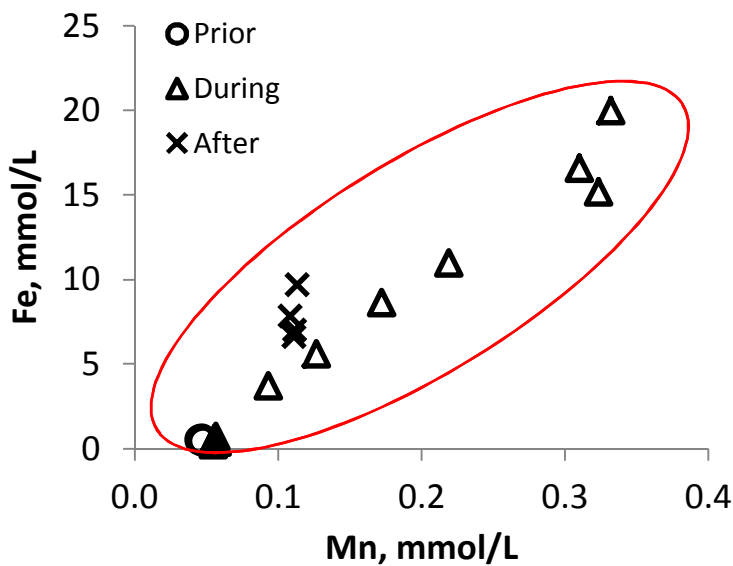
Monitoring Well Sampled During Injection



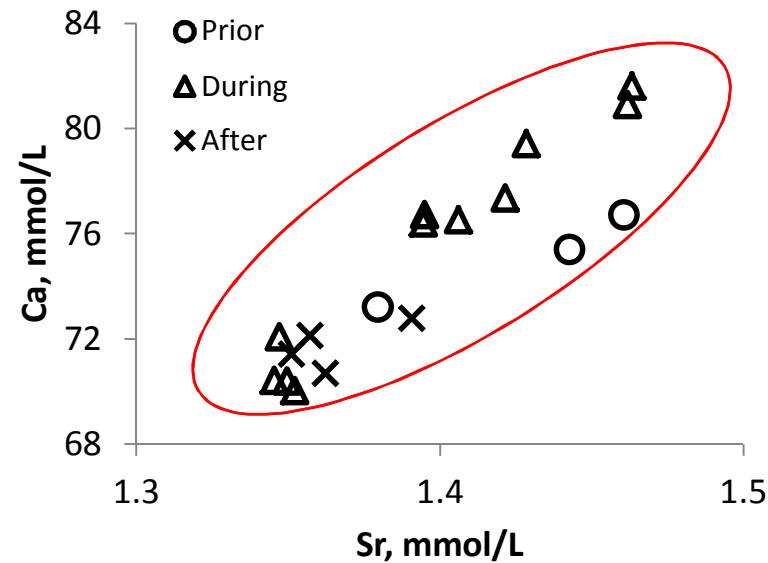
- A subset of samples collected from the monitoring well during CO₂ injection.
- Fe increases continuously.
- Ca and Sr increase, then decrease, potentially indicates full dissolution of the Ca-phase.



Results: Calcium and iron in brine samples

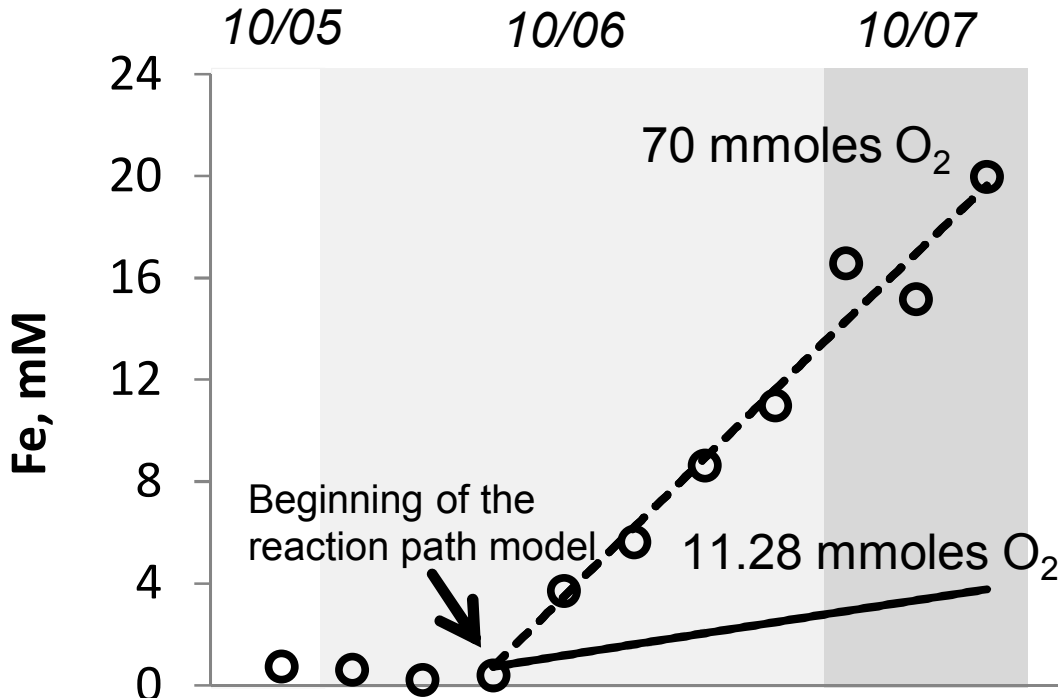


- Positive correlation - iron and manganese - indicate the same source - Mn-enriched pyrite found in the Frio "C" sandstones.
- No correlation between Fe and S - pyrite dissolution is an incongruent process.¹



[1] Descostes et al., 2004

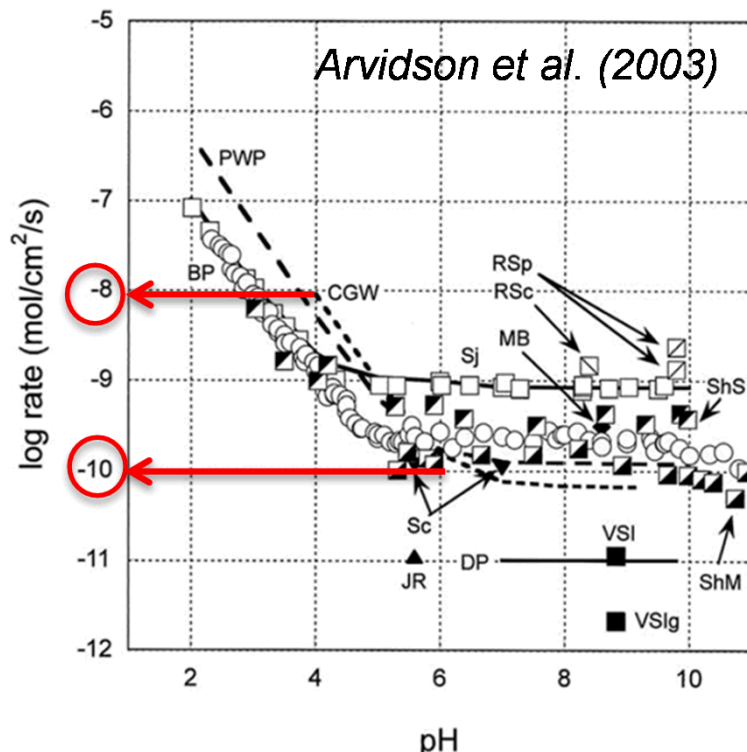
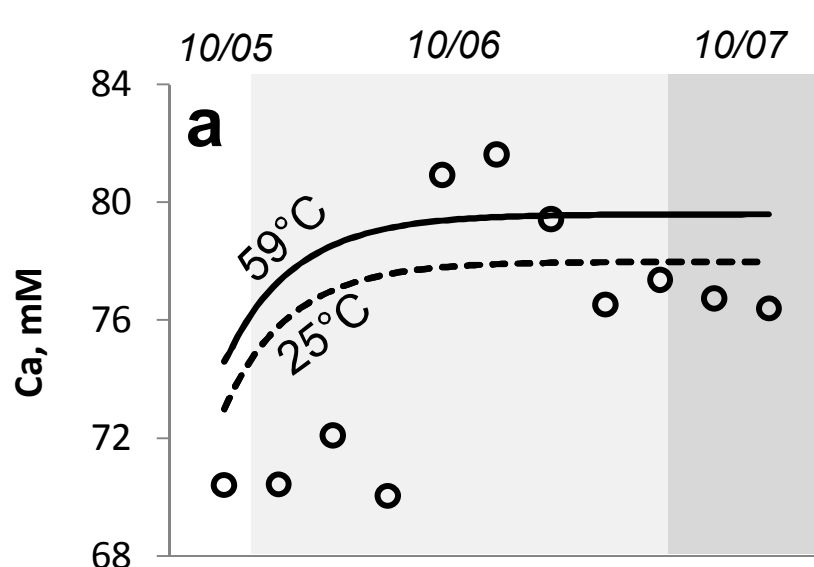
Results: Pyrite dissolution model



- Dissolution of pyrite by introduced O₂ – common impurity gas in CO₂ streams (3-12 vol. %).¹
- The reaction path models were started at the onset of Fe²⁺ increase in the monitoring well samples.
- The reaction path models assume Fe is released during simple pyrite dissolution, the mass of available pyrite is set at 10 g, and temperature = 25°C.



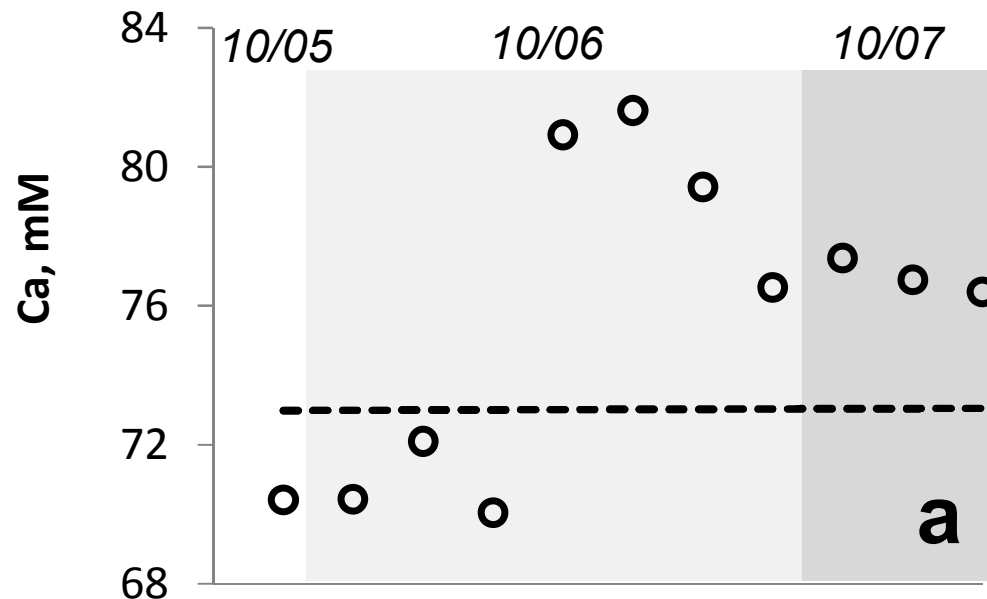
Results: Calcite dissolution and associated uncertainties



- (a) Reaction path models assume Ca is released during calcite dissolution, the mass of available calcite, dissolution rate constant $k = 10^{-8} \text{ mol cm}^{-2} \text{ sec}^{-1}$,
- (b) Uncertainty: dashed lines - models calculated at 25°C, solid lines - at 59°C. Group "A" = 9 g CaCO₃, $k = 10^{-8} \text{ mol cm}^{-2} \text{ sec}^{-1}$, group "B" - 9 g CaCO₃, $k = 10^{-10} \text{ mol cm}^{-2} \text{ sec}^{-1}$, group "C" - 0.09 g CaCO₃, $k = 10^{-8}$ and $10^{-10} \text{ mol cm}^{-2} \text{ sec}^{-1}$.

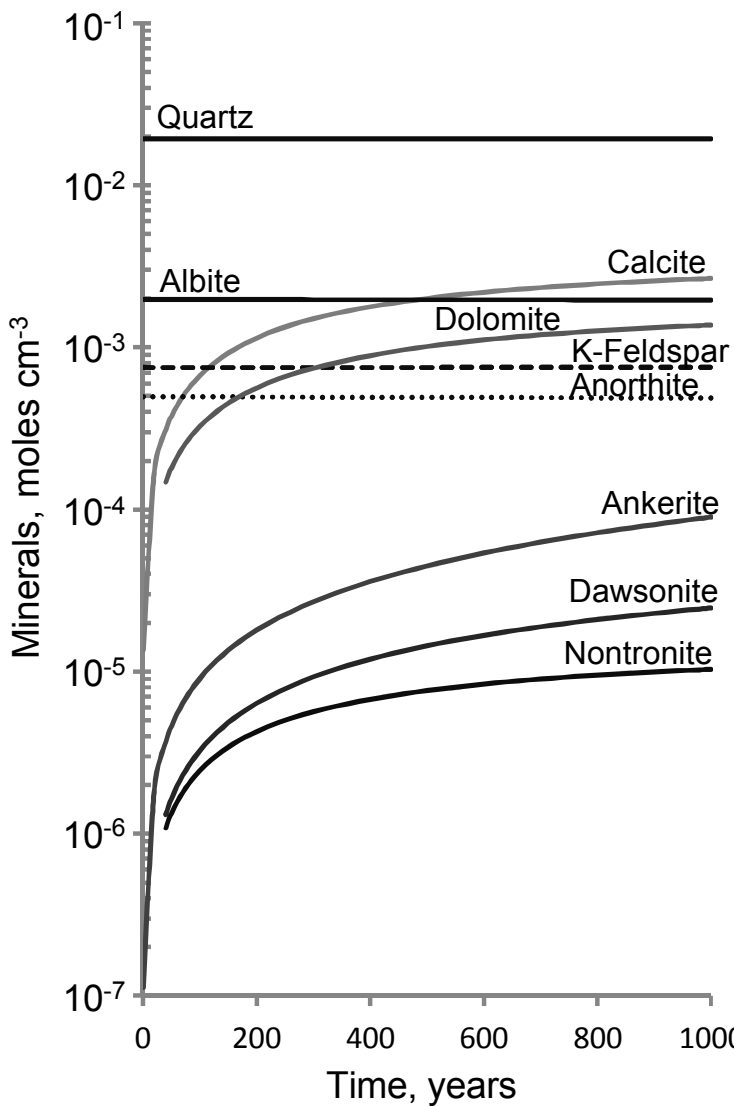


Results: Anorthite dissolution model

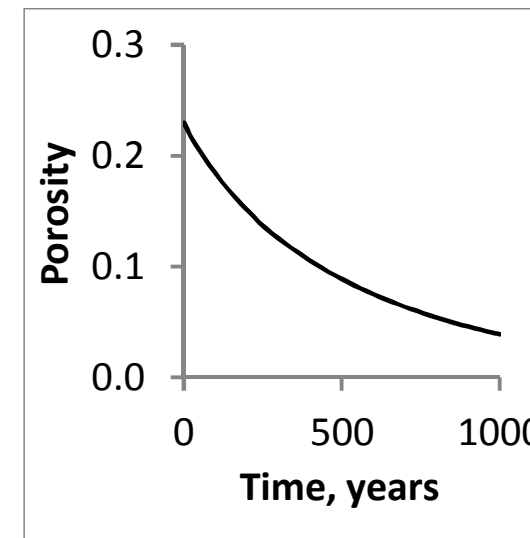


- This reaction path model assumes Ca is released during kinetically controlled anorthite dissolution.
- The mass of available anorthite was set at 35 g and at 350 g, and the calculated concentrations of dissolved calcium overlap, anorthite dissolution rate constant $k = 2.1 \times 10^{-14} \text{ mol cm}^{-2} \text{ sec}^{-1}$, temperature is set at 25°C.

Results: Reactive flow model



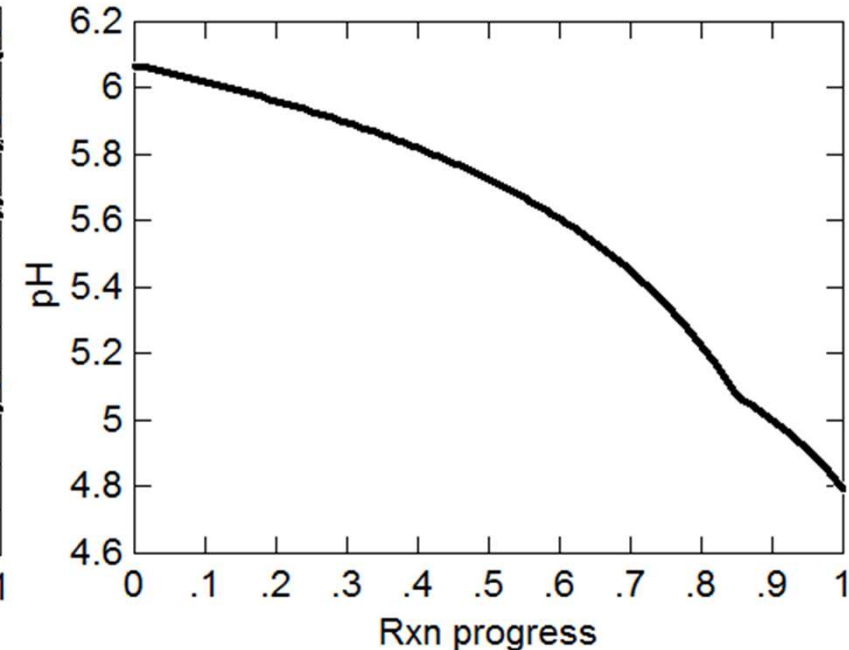
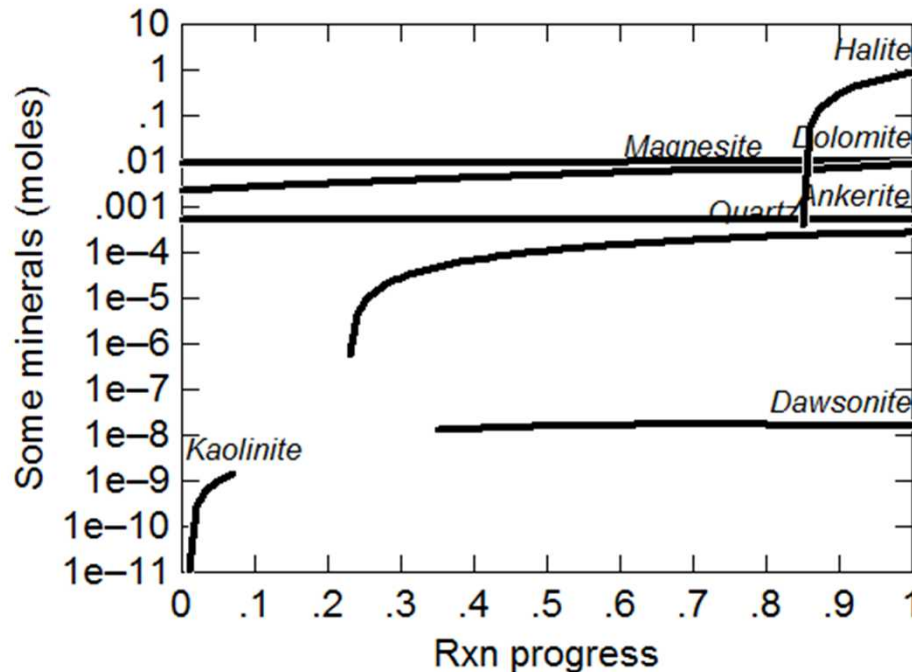
- Based on the path of reaction models, dissolution of **pyrite** and trace amounts of **calcite** are included.
- Precipitation of carbonates: dolomite, ankerite, dawsonite, and calcite, as well as smectite clay (nontronite), significant after 10 years.
- Predicted decrease in porosity: from 23 to 4%.





Precipitation due to dehydration (near wellbore)

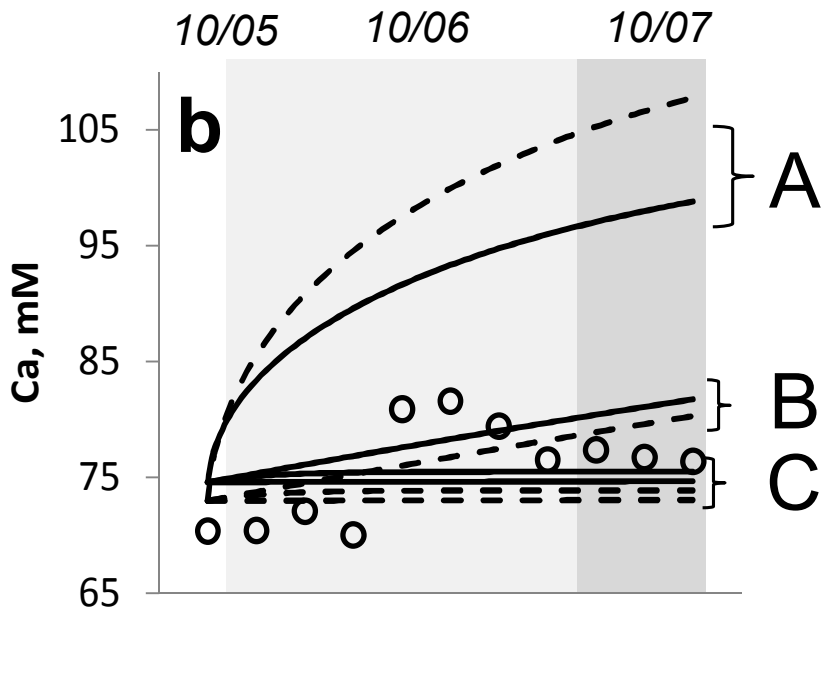
Input: Aqueous species + Calcite. Assume brine/CO₂ did NOT equilibrate before dehydration by scCO₂. Precipitation - allowed. Single reactant -900 g H₂O



- Oversaturated minerals are allowed to precipitate before reaction;
- **Prediction:** pH decreases to 4.8, halite, dolomite, magnesite, quartz, and dawsonite precipitate.

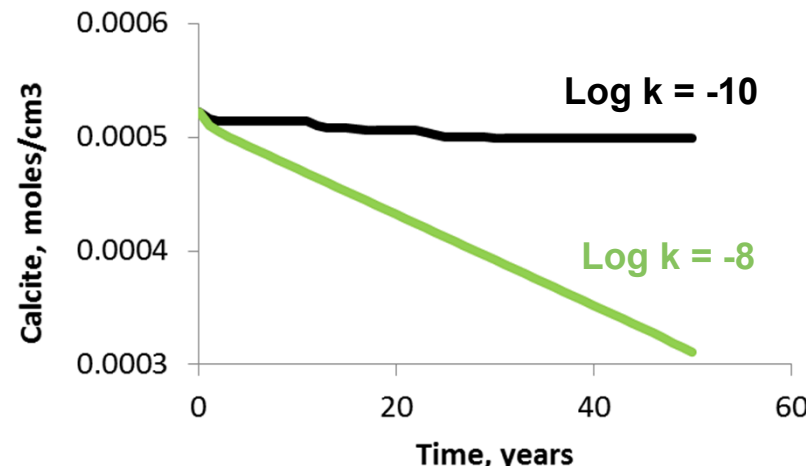
Calcite dissolution modeling uncertainty

Trace amounts of calcite in the reservoir rocks:



Significant amounts of calcite in the reservoir rocks

- 2 vol. % of calcite
- Reaction with NaCl brine and dissolved CO₂, final pH 4.8.



- Calcite dissolution over 50 years differs by 60%.

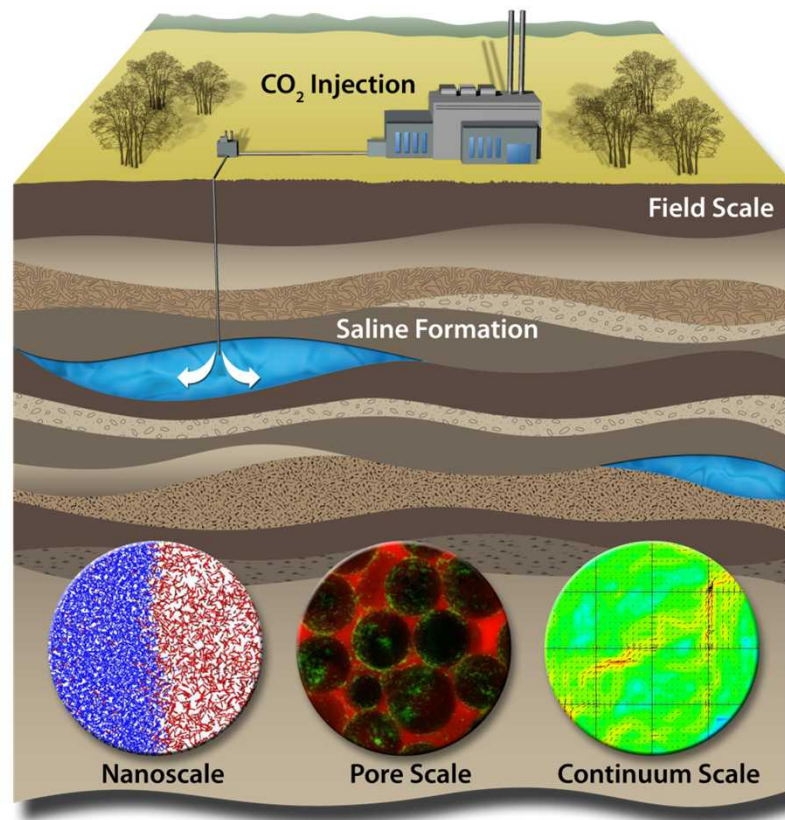
Conclusions

- Increasing Ca and Sr concentrations in the monitoring well are best matched by the dissolution of trace amounts of calcite, whereas the dissolution kinetics of anorthite is too slow to account for the levels of observed calcium release.
- Pyrite dissolution is a likely source of iron and manganese in the brine collected in the monitoring well.
- 1D reactive flow model indicates mineral precipitation in the Frio Formation “C” sandstone as the system progresses towards chemical equilibrium during a 1000 year period. Significant amounts of calcite, dolomite, ankerite, and dawsonite, as well as smectite clay (nontronite) are expected to precipitate, with a corresponding significant loss of porosity of ~19 %.

Future Work

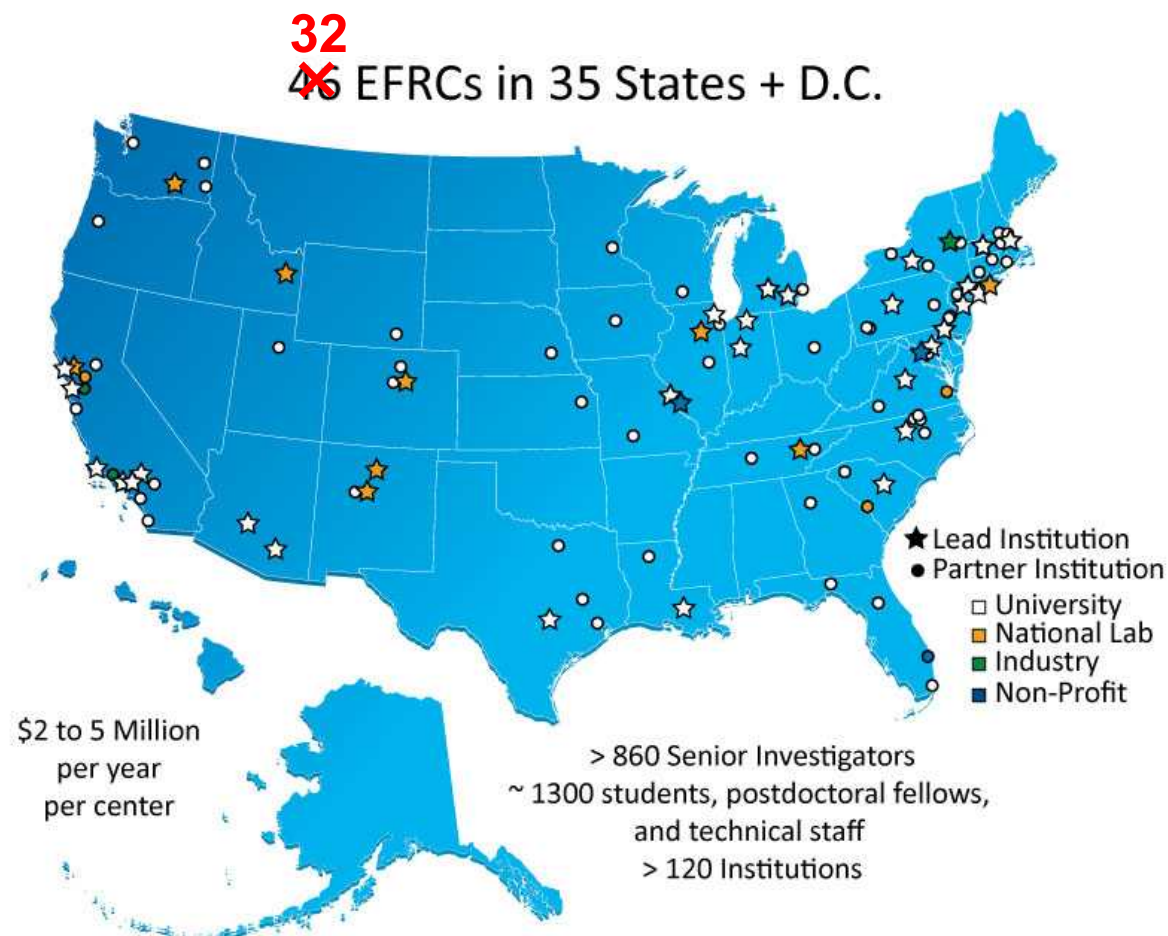
- Laboratory experiments at pressures and temperatures typical for GCS to investigate coupled geochemical and geomechanical response of representative cap rock (shale) and brine systems during reaction with scCO₂.

Overview of the Center for Frontiers of Subsurface Energy Security (CFSES)



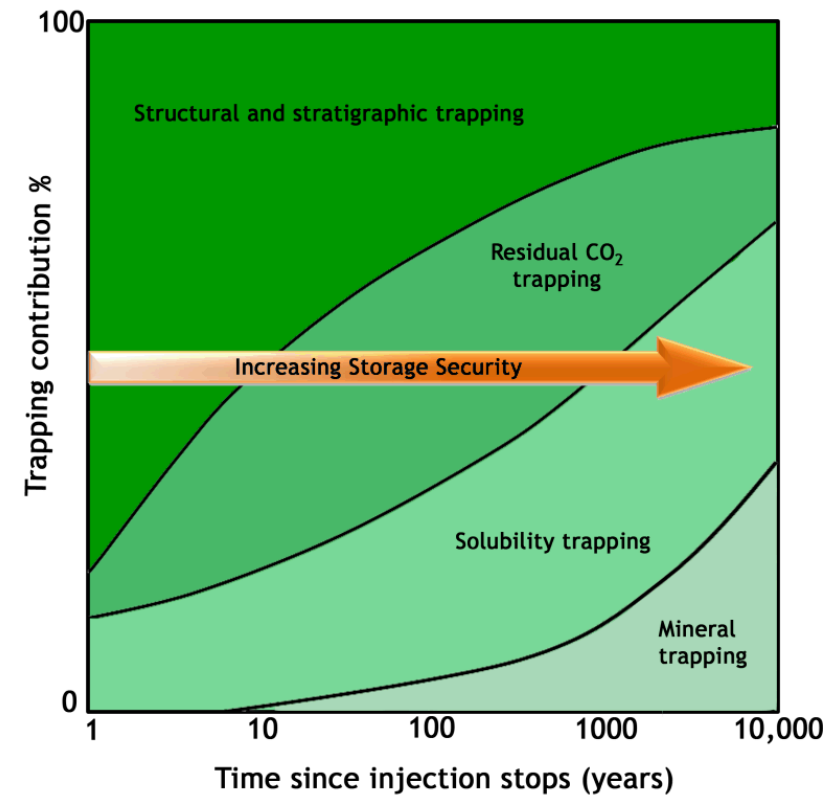
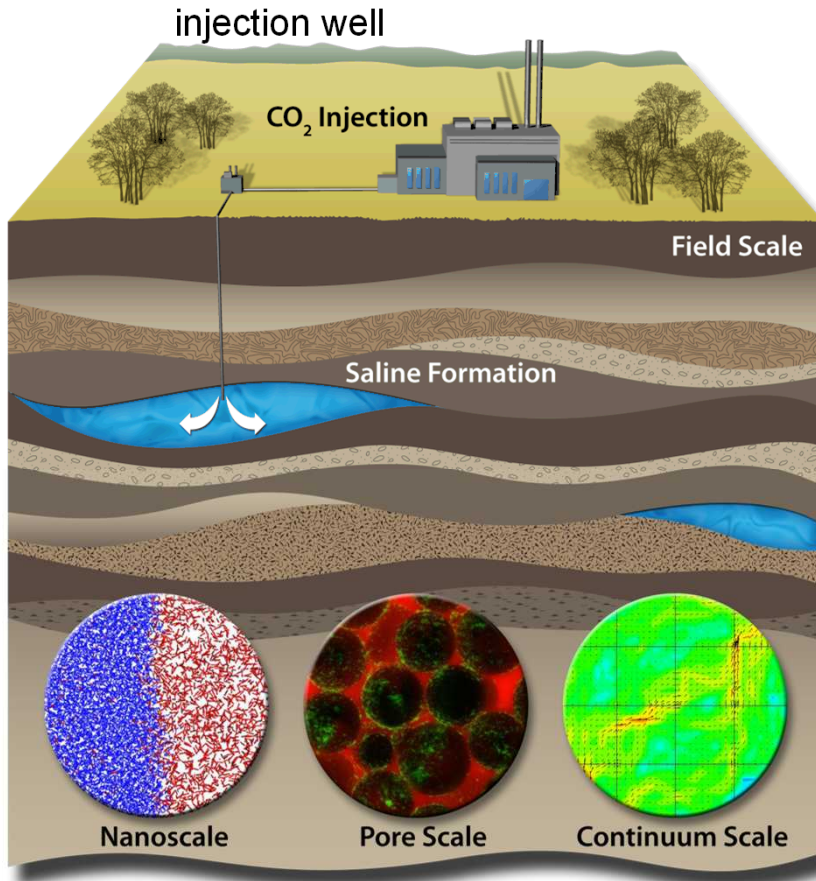
The Energy Frontier Research Centers Aim to Accelerate Discovery Science for Energy Technologies

- Round 1: 2009 - 2014
- CFSES is one of 2 geosciences related EFRC
- Renewal started 08/2014
- 4 year program
- **CFSES is one of 3 geosciences related EFRCs**



Ensure Safe Storage of CO₂

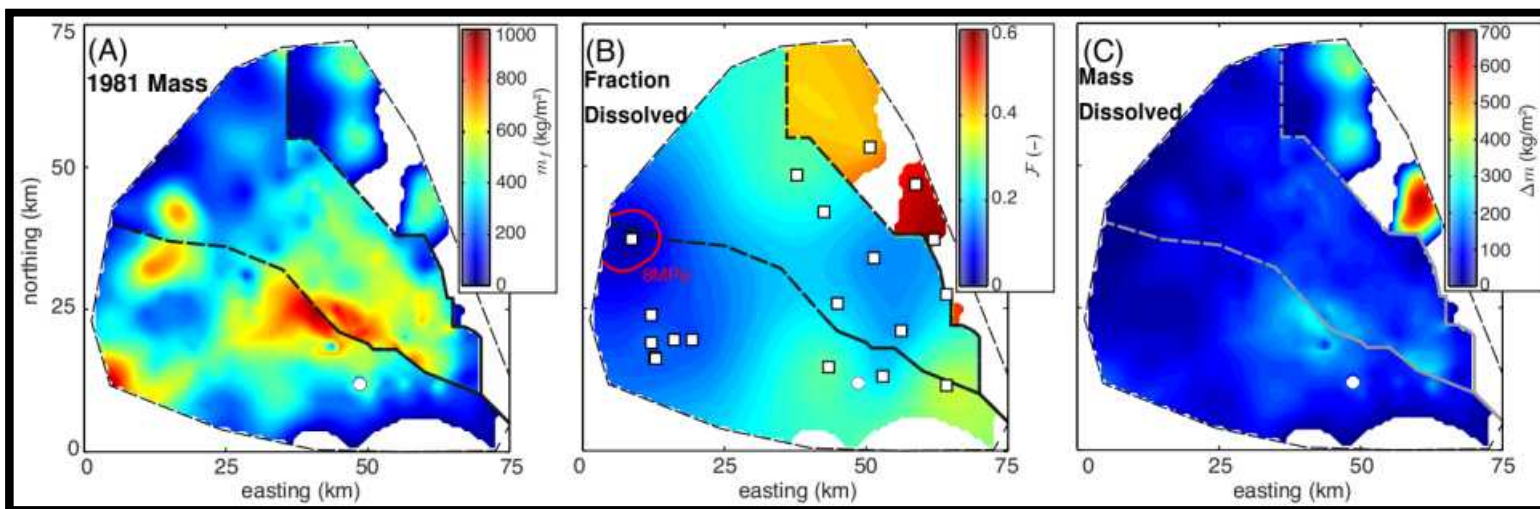
The Center for Frontiers of Subsurface Energy Security (CFSES) is pursuing scientific understanding of multi-scale, multi-physics processes to ensure safe and economically feasible storage of carbon dioxide and other byproducts of energy production without harming the environment.



Natural analogs: long-term dissolution of stored CO₂

Storing gigatons of CO₂ in deep saline aquifers in a few decades represents a substantial disequilibrium of the subsurface environment. Because the CO₂ phase is buoyant but brine becomes more dense when saturated with dissolved CO₂, a central question for GCS security is the rate of dissolution of a CO₂ plume after it has been emplaced.

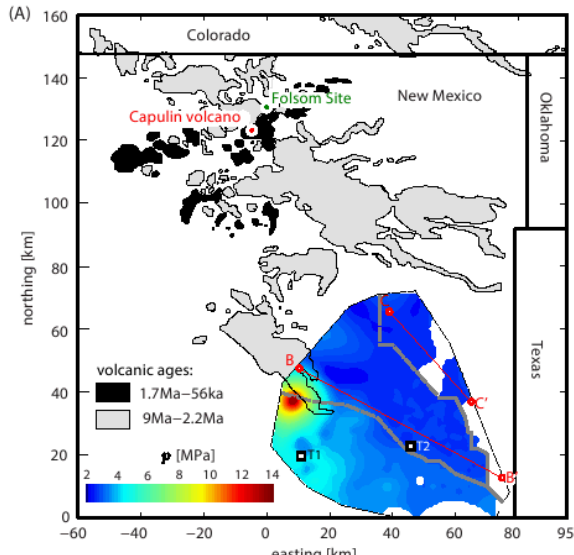
The Bravo Dome reservoir demonstrates that long-term, safe geological CO₂ storage is possible.



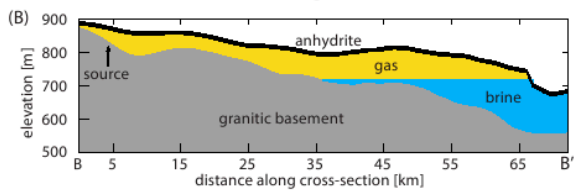
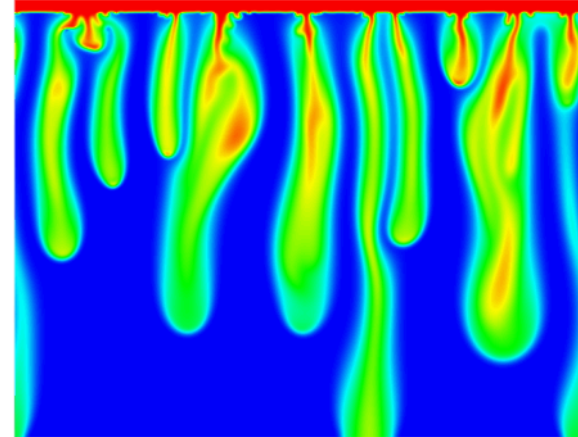
- A) *Mass of CO₂ per unit area in the Bravo Dome reservoir in 1981.*
- B) *Map of the local fraction of CO₂ dissolved.*
- C) *Map of the local change in the mass of CO₂ per unit area.*

- Estimated 22% of the emplaced CO₂ has dissolved into the brine over 1.2 My. Estimated a convective dissolution rate of 0.1 g/(m²y)

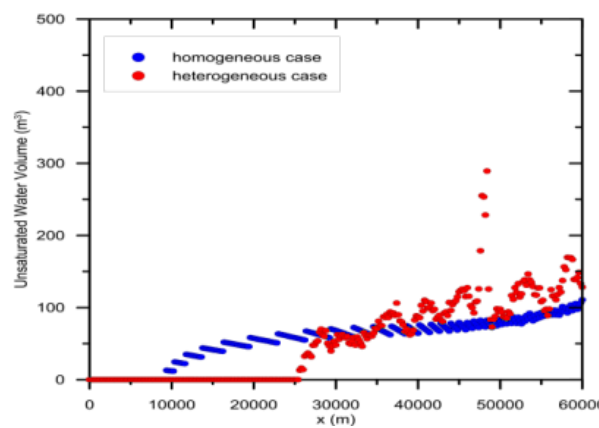
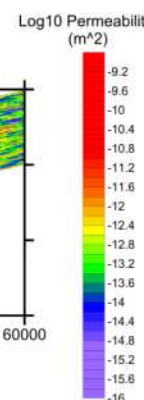
How Important is CO₂ Dissolution?



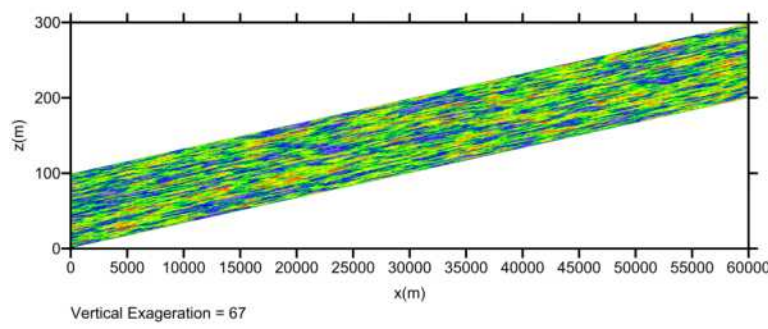
- **Bravo Dome Site: 360Mt CO₂ dissolved over 1.5Ma.**
- **Convectively driven dissolution flux may be roughly 3x larger than current estimates.**



Goal: Improved estimates of the long-term dissolution rate of CO₂ into brine by including the two-phase region above the gas-water contact in model simulations. Long-term dissolution rate can be enhanced by greater than 3 times the dissolution rates derived from ignoring the capillary transition zone.

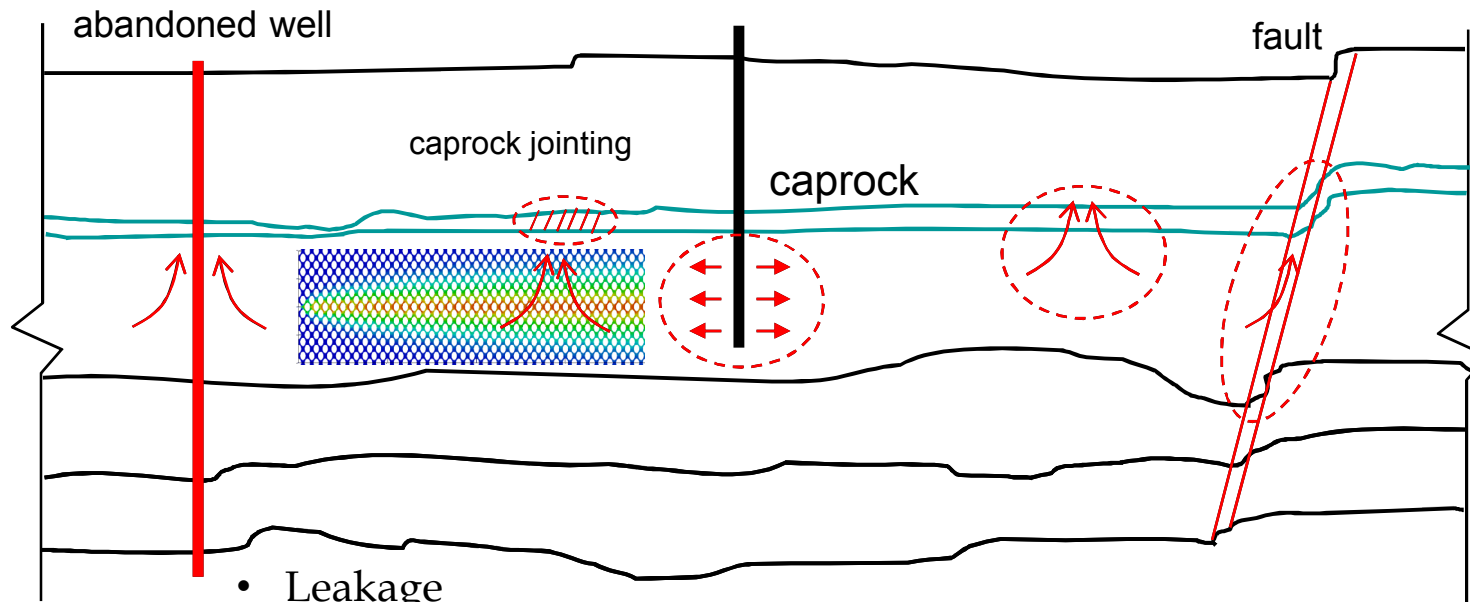


Dissolution is enhanced by heterogeneity.



Ensure Safe Storage of CO₂

CFSES will pursue scientific advances to understand chemico-mechanical coupling between supercritical CO₂ and clay minerals, understand and predict modes and fluxes of reactive CO₂ migration, and design, develop and apply novel materials that will alter fluid-assisted perturbations in heterogeneous geomaterials.



- Leakage
 - Wellbores
 - Faults
- Injection induced damage
- Brine migration to overlying aquifers
- Induced seismicity

Integrating Research Themes with Challenges



	Challenge 1: Sustaining large storage rates	Challenge 2: Using pore space with unprecedented efficiency	Challenge 3: Controlling undesired or unexpected behavior
Theme 1: Fluid-Assisted Geomechanics	<ul style="list-style-type: none">Single Fracture propagation and cohesive zone modelingPhase-field modeling	<ul style="list-style-type: none">Single Fracture propagation and cohesive zone modeling	<ul style="list-style-type: none">Bulk rock strengthening/weakening evaluation
Theme 2: Multifluid Geochemistry	<ul style="list-style-type: none">Caprock chemical and mechanical stability	<ul style="list-style-type: none">Bravo Dome brine-gas mass transferChemistry at the fluid-fluid interface	<ul style="list-style-type: none">Caprock chemical and mechanical stabilityReactions of CO₂ with clay minerals
Theme 3: Buoyancy-Driven Multiphase Flow	<ul style="list-style-type: none">Meter-scale experimentsCore-scale X-ray CT experiments	<ul style="list-style-type: none">Meter-scale experimentsCore-scale X-ray CT experimentsMesoscale modeling and invasion-percolation modelingGanglion dynamics modeling	<ul style="list-style-type: none">Nanoparticle experiments

Center For Frontiers of Subsurface Energy Organizational Structure



EAB

Steve Bryant
Charles Christopher
Don DePaolo
Derek Elsworth
Robert Finley
Kurt House
Jean Roberts

Management Team

Larry Lake – Director
Marianne Walck – Associate Director
Susan Altman, Hilary Olson – Assistant Directors

Administrative Associate

Barb Messmore

THEME 1: FLUID-ASSISTED GEOMECHANICS

Theme Leads:

Tom Dewers **Sanjay Srinivasan**
M. Balhoff, J. Bishop, P. Eichhbul,
N. Espinoza, N. Hayman, M.
Hesse, A. Ilgen, M. Martinez,
M. Wheeler, H. Yoon

THEME 2: MULTIFLUID GEOMECHANICS

Theme Leads:
Randall Cygan **Marc Hesse**
P. Bennett, B. Cardenas,
O. Ghattas, A. Ilgen,
C. Tenney, C. Yang

THEME 3: BUOYANCY-DRIVEN MULTIPHASE FLOW

Theme Leads:
Tip Meckel, **Mario Martinez**
B. Cardenas, D. DiCarlo, N.
Espinoza, S. Hovorka, K.
Johnston, Y. Wang, H. Yoon, C.
Huh

Acknowledgments

People

Susan Hovorka, BEG – Frio-I chemistry data

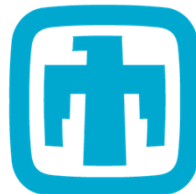
Carlos Jove-Colon, SNL – Thermodynamic database

Katherine Klise, SNL – Thermodynamic database conversion

Susan J. Altman, SNL – CFSES overview slides

Funding

Center for Frontiers of Subsurface Energy Security, an Energy Frontier Research Center funded by the U.S. Department of Energy, Office of Science, Office of Basic Energy Sciences under Award Number DE-SC0001114.



Sandia
National
Laboratories



U.S. DEPARTMENT OF
ENERGY

Office of
Science

Center for Frontiers of
Subsurface Energy
Security



CFSES